Magnetoresistive Properties of Zn1−xCoxFe2O4 Ferrites

ARTICLE *in* JOURNAL OF MAGNETISM AND MAGNETIC MATERIALS · MARCH 2008

Impact Factor: 1.97 · DOI: 10.1016/j.jmmm.2007.11.009

3 AUTHORS, INCLUDING:

A.K.M. Akther Hossain
Bangladesh University of Engineering and …
84 PUBLICATIONS **536** CITATIONS
SEE PROFILE

Hitoshi Tabata
The University of Tokyo
211 PUBLICATIONS **6,949** CITATIONS
SEE PROFILE

Available online at www.sciencedirect.com
ScienceDirect
Journal of Magnetism and Magnetic Materials 320 (2008) 1157–1162
Journal of magnetism and magnetic materials
www.elsevier.com/locate/jmmm

Magnetoresistive properties of $Zn_{1-x}Co_xFe_2O_4$ ferrites

A.K.M. Akther Hossain[a,*], H. Tabata[b], T. Kawai[c]

[a]Department of Physics, Bangladesh University of Engineering and Technology, Dhaka 1000, Bangladesh
[b]Department of Bioengineering and Electronic Engineering, School of Engineering, The University of Tokyo, 7-3-1 Hongo, Bunkyo-ku, Tokyo 113-8656, Japan
[c]Institute of Scientific and Industrial Research, Osaka University, 8-1 Mihogaoka, Ibaraki, Osaka 567-0047, Japan

Received 6 July 2007; received in revised form 11 October 2007
Available online 17 November 2007

Abstract

The magnetic and magnetoresistive properties of spinel-type $Zn_{1-x}Co_xFe_2O_4$ ($x = 0$, 0.2 and 0.4) ferrites are extensively investigated in this study. A large negative magnetoresistance (MR) effect is observed in $Zn_{1-x}Co_xFe_2O_4$ ferrites of spinel structure. These materials are either ferrimagnetic or paramagnetic at room temperature, and show a spin-(cluster) glass transition at low temperatures, depending on the chemical compositions. The MR curves as a function of magnetic fields, MR(H), are parabolic at all temperatures for paramagnetic polycrystalline $ZnFe_2O_4$. The MR for $ZnFe_2O_4$ at 110 K in the presence of 9 T applied magnetic field is 30%. On the other hand, MR(H) are linear for $x = 0.2$ and 0.4 ferrimagnetic $Zn_{1-x}Co_xFe_2O_4$ samples up to 9 T. The MR effect is independent of the sintering temperatures, and can be explained with the help of the spin-dependent scattering and the Yafet–Kittel angle of $Zn_{1-x}Co_xFe_2O_4$ mixed ferrites.

PACS: 75.70.P; 75.50.Gg

Keywords: Magnetoresistance; Saturation magnetization; Grain size; Transition temperature

1. Introduction

Spinel-type ferrites have been the subject of intense research interest because of their potential application in many electronic devices and also from the point of view of fundamental physics. According to their crystal structure, spinel-type ferrites have natural superlattice. They have tetrahedral A sites and octahedral B sites in AB_2O_4 crystal structure. They show various magnetic properties depending on the composition and cation distribution. Various cations can be placed in the A sites and B sites to tune its magnetic properties. Depending on the A site and B site cations, ferrimagnetic, antiferromagnetic, spin-(cluster) glass and paramagnetic behavior are observed in these spinel ferrites [1–4]. Due to their amazing magnetic and electric properties, spinel ferrites have become a subject of both theoretical and experimental investigation for application purposes [5–9]. The ferrites have been found to be one of the most versatile systems for general use in many devices. They represent a wide choice of permeability, coercive force and magnetic and electric losses [10]. Although numerous spinel compounds have been studied earlier, a complete understanding of the complex magnetic behavior arising from the change in cation concentration is yet to be revealed.

Magnetoresistance (MR) refers to a change of electrical resistance in the presence of magnetic field. This effect has been most extensively studied in perovskite $R_{1-x}D_xMnO_3$, where R is a rare earth cation (e.g. La, Y, Gd, etc.) and D is a divalent cation (e.g. Ca, Sr, Ba, etc.). Generally, in these compounds, the material undergoes a phase transition from semiconducting (paramagnetic) to metallic (ferromagnetic) phase [11]. The intrinsic MR effect depends on

*Corresponding author. Tel.: +880 2 966 5613; fax: +880 2 861 3046.
E-mail address: akmhossain@phy.buet.ac.bd (A.K.M. Akther Hossain).

0304-8853/$ - see front matter © 2007 Elsevier B.V. All rights reserved.
doi:10.1016/j.jmmm.2007.11.009

the chemical composition, transition temperature (T_c) and crystal structure, etc. In addition to this intrinsic MR, the polycrystalline manganites also show low-temperature MR related to the microstructure of the sample [12]. A negative MR effect was observed by Gausepohl et al. [13] in perovskite $SrRuO_3$ and La and Fe substituted $SrRuO_3$ by Mamchik and Chen [14]. There are also some reports of negative MR in spinel-type Fe_3O_4 [15,16] and Cr-based chalcogenide spinels [17]. The MR observed in these samples was explained with the help of either spin-dependent tunneling or some mechanisms of atomic-level spin valves. Hossain et al. [18] reported large negative MR in Yafet–Kittel (YK)-type $Zn_{1-x}Ni_xFe_2O_4$. If the Zn content is greater than 0.5, the B site cations are no longer collinear. The spins of the B site cations are canted and made a certain angle. This angle is 90° for $ZnFe_2O_4$. The ferrites with canted B sites cations are called the YK-type ferrites. Normally, the ferrites are high resistive and the MR effect of these high-resistive ferrites are fascinating. From our previous study, it was observed that the ferrites with collinear B site cations show negligible MR. For this reason, in this research we intend to investigate three representative compositions of $Zn_{1-x}Co_xFe_2O_4$ ($x = 0$, 0.2 and 0.4). In this paper the magnetic and large negative magnetoresistive properties of these highly resistive YK-type $Zn_{1-x}Co_xFe_2O_4$ spinel ferrites are described.

2. Experimental

Various $Zn_{1-x}Co_xFe_2O_4$ ($x = 0$, 0.2 and 0.4) compositions were synthesized by the standard solid-state reaction technique from stoichiometric amounts of Fe_2O_3, ZnO and CoO of 99.99% purity. Appropriate amounts of oxides were mixed thoroughly and then calcined at 1273 K for 24 h. The calcined powders were ground to a fine powder. The disc-shaped samples prepared from $Zn_{1-x}Co_xFe_2O_4$ were sintered in air at 1573 K for 5 h. Pellets prepared from $ZnFe_2O_4$ powders were sintered at various temperatures (1373–1573 K) for obtaining samples of various microstructures (grain size). The microstructures of the samples were investigated with a high-resolution optical microscope. The phase purity was checked by powder X-ray diffraction using CuKα radiation. The electrical resistance measurements were carried out using Physical Property Measurement system (PPMS model 6000; Quantum design Co. Ltd.). The dc resistivity (ρ) of different $Zn_{1-x}Co_xFe_2O_4$ samples was measured by a standard four-point probe and the van der Pauw technique [19,20]. For MR measurements, the magnetic field was applied perpendicular to the current flow in the sample. The magnetization (M) measurements were made on pieces of the samples (approximate dimensions $2 \times 1 \times 1\,mm^3$) using the Superconducting Quantum Interface Device (SQUID) magnetometer (MPMS-5S; Quantum design Co. Ltd.).

3. Results and discussion

3.1. Lattice parameters, density, porosity and grain size of $Zn_{1-x}Co_xFe_2O_4$

The room temperature X-ray diffraction patterns for various $Zn_{1-x}Co_xFe_2O_4$ samples are shown in Fig. 1. The X-ray diffraction patterns show that all the samples are single phase with spinel structure. The samples are assigned to a pseudo-cubic structure. The values of lattice constants for all samples are given in Table 1. It was observed that the lattice constant slightly decreases as the Co concentration increases. This is probably due to variation of ionic sizes of the Zn^{2+} and Co^{2+} cations. The ionic size of Zn^{2+} (0.74 Å) is higher than that of Co^{2+} (0.72 Å) [21]. A similar behavior was observed by other authors [1,3,4,18]. The theoretical density, d_{th}, was calculated using the expression

$$d_{th} = \frac{8 \times \text{molecular weight}}{N_A a_0^3},$$

where N_A is the Avogadro's number and a_0 is the lattice constant. The porosity was calculated using the relation

$$P = \left(\frac{d_{th} - d_B}{d_{th}}\right) \times 100\%,$$

where d_B is the bulk density measured by the formula

$$d_B = \frac{\text{mass of the sample}}{\text{volume of the sample}}.$$

The values of the d_{th}, d_B and P for all samples are also tabulated (Table 1). The porosity of the sample increases as the Zn content decreases in these polycrystalline ferrite samples. This is probably due to the enhancement of the grain size of the samples as the Zn content is higher as shown in Fig. 2. The values of the average grain size (measured by linear intercept technique) are provided in Table 1.

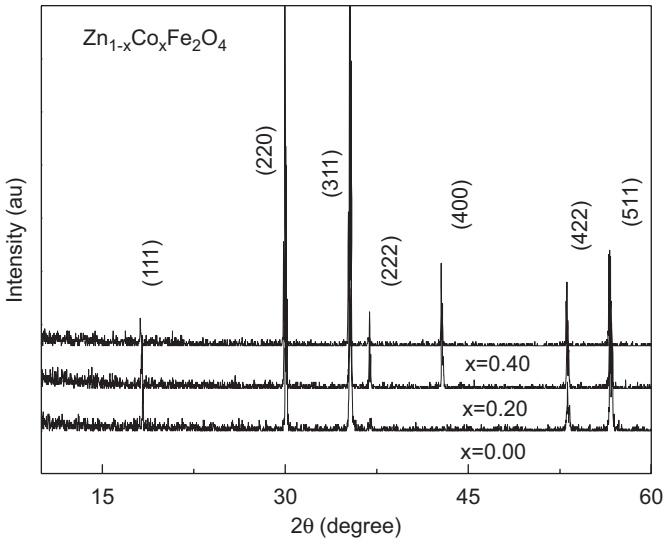

Fig. 1. Room temperature X-ray diffraction patterns for the various $Zn_{1-x}Co_xFe_2O_4$ taken with CuKα radiation.

Table 1
The lattice parameters, density, porosity, resistivity at room temperature and average grain size for various $Zn_{1-x}Co_xFe_2O_4$ polycrystalline samples

Sample composition	a_0 (Å)	d_{th} (g/cm^3)	d_B (g/cm^3)	P (%)	ρ (300 K) Ω m	Average grain size (μm)
$ZnFe_2O_4$	8.4710±0.0012	5.268	4.912	7	11	60
$Zn_{0.80}Co_{0.20}Fe_2O_4$	8.4644±0.0011	5.252	4.698	11	36	12
$Zn_{0.60}Co_{0.40}Fe_2O_4$	8.4528±0.0012	5.245	4.622	12	43	8

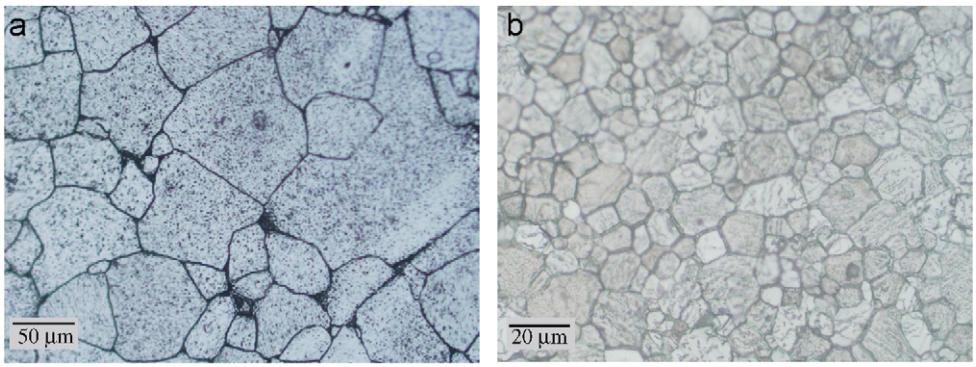

Fig. 2. Optical micrographs for (a) $ZnFe_2O_4$ and (b) $Zn_{0.60}Co_{0.40}Fe_2O_4$ polycrystalline samples.

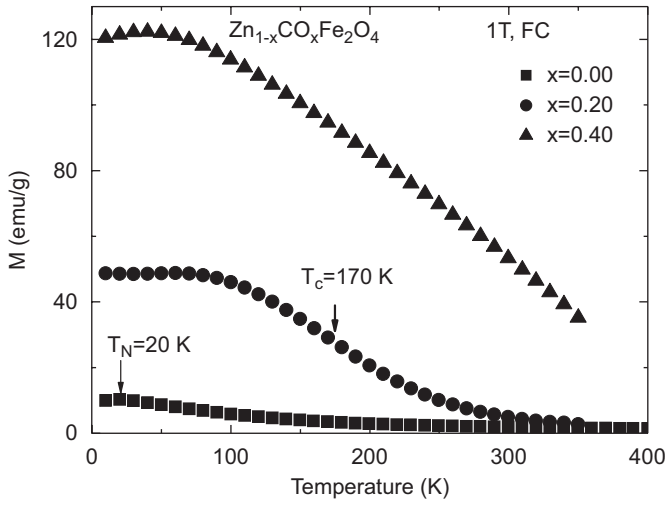

Fig. 3. Temperature dependence of magnetization curves for the various $Zn_{1-x}Co_xFe_2O_4$ samples. Data were taken in the presence of 1 T applied magnetic field in field-cooled condition.

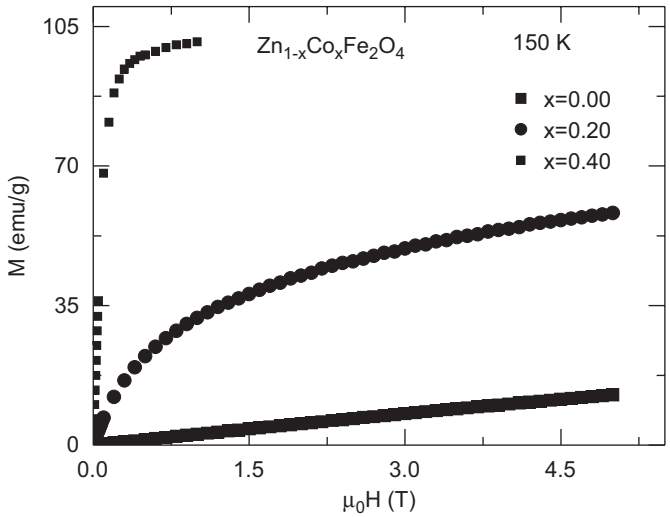

Fig. 4. Magnetization as a function of applied magnetic field curves for the various $Zn_{1-x}Co_xFe_2O_4$ samples.

3.2. Magnetic properties of $Zn_{1-x}Co_xFe_2O_4$

Fig. 3 shows the magnetization as a function of temperature, $M(T)$, for various $Zn_{1-x}Co_xFe_2O_4$ samples. The data were recorded in the presence of 1 T applied magnetic field using the field-cooled method. It is observed that the $x = 0$ sample is paramagnetic, and this sample undergoes an antiferromagnetic transition at $T_N = 20$ K. The $x = 0.20$ sample is ferromagnetic below 170 K. These results agree with those obtained by Petitt and Forester [24] by Mossbauer spectroscopy. The other sample ($x = 0.4$) is ferromagnetic at room temperature and also at 400 K, showing T_c above 400 K.

Fig. 4 shows the variation of magnetization as a function of applied magnetic field, $M(H)$, for various $Zn_{1-x}Co_xFe_2O_4$ samples at 150 K. The $x = 0$ sample shows a linear magnetization behavior indicating that the sample is paramagnetic. On the other hand, $x = 0.20$ and 0.40 samples show nonlinear magnetization. The increase of magnetization up to 5 T applied magnetic field shows that these samples are not a collinear ferrimagnet. This could also be viewed as an evidence for incomplete long-range ordering among magnetic ions. No saturation is observed in the presence of 5 T applied magnetic field.

Fig. 5 shows M–H loops at 10 K for various $Zn_{1-x}Co_xFe_2O_4$ samples with different Co contents. From these

loops it is found that the samples with $x = 0.2$ and 0.4 are hard ferrimagnets. These materials show a considerable hysteresis. The coercive field is higher for the $x = 0.2$ sample than for the $x = 0.4$ sample.

Fig. 6 shows the number of Bohr magneton (μ_B) as a function of Co content. The μ_B was calculated from M (1 T) value. Theoretical values of Co content dependence of μ_B, for $Zn_{1-x}Co_xFe_2O_4$, are also shown in Fig. 6 for collinear ferrimagnetisms. The collinear ferrimagnetism may be observed for higher Co concentrations ($x > 0.50$). The lower concentration of Co ($x < 0.50$) renders a strong deviation from collinear ferrimagnetism. From the M–H curves, we also see that the sample with low Co content does not show saturation even in the presence of 5 T applied magnetic field (Fig. 4). Bhowmik and Ranganathan [25] showed that the magnetization of $Zn_{0.80}Co_{0.20}Fe_2O_4$ sample is not saturated even in the presence of 12 T applied magnetic field.

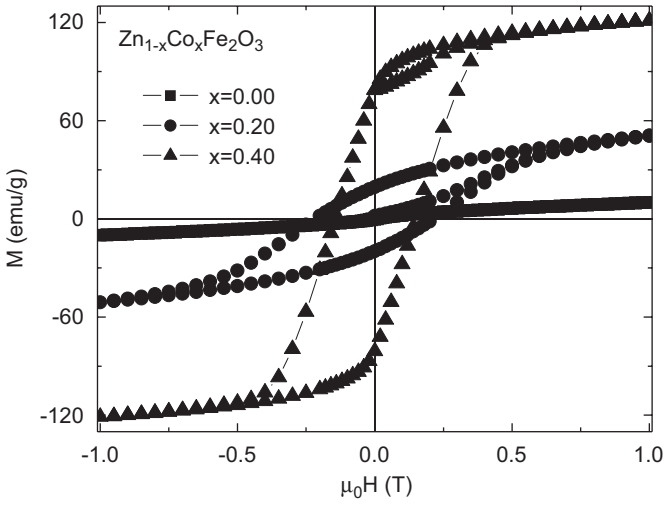

Fig. 5. The M–H loops for the various $Zn_{1-x}Co_xFe_2O_4$ samples at 10 K.

3.3. Magnetoresistance of $Zn_{1-x}Co_xFe_2O_4$

Due to the high resistivity of the samples [e.g. $\rho(300\,\mathrm{K}) = 11$, 36 and 43 Ω m for $x = 0$, 0.2 and 0.4, respectively] and the limitation of current source of the measuring system, ρ was measured between 400 and 110 K as shown in Fig. 7. It is found that the $\rho(T)$ increases as the Co content increases, and $\rho(T)$ for all samples follows $\rho(T) \propto T\exp(E_h/k_BT)$, where E_h is the polaron hopping energy (fits are shown in the inset of Fig. 7). The $\rho(H)$ were measured at various temperatures in the form of a loop, from 0 to +9 T, to −9 T and then from −9 to +9 T magnetic field. From these results, MR(H) was calculated from the following relation:

$$\mathrm{MR}(\%) = \frac{\rho(H=0) - \rho(H)}{\rho(H=0)} \times 100. \quad (1)$$

Fig. 8(a) shows the MR(H) loops for the $ZnFe_2O_4$ at various temperatures. For this sample, 30% MR is observed at 110 K in the presence of 9 T field. The MR is not saturated at 9 T, but increases to about 4.5%/T at this temperature. Results of M measurements exhibit that this sample undergoes paramagnetic to antiferromagnetic transition at $T_N = 20$ K. However, from the $M(H)$ measurement, a nonlinear behavior is observed at low magnetic field at 200 K, indicating that the sample might have short-range ordering or a number of ferromagnetic clusters embedded in the paramagnetic matrix. The MR behavior observed in this sample seems to be originated from these small clusters, magnetic polaron and randomly aligned paramagnetic spins. The clusters as well as randomly aligned paramagnetic spins tend to align towards an external magnetic field. Hence, the carrier suffers less scattering than that in the absence of magnetic field. The shape of the MR(H) for $ZnFe_2O_4$ resembles that for the MR(H) in the paramagnetic regime for the manganite

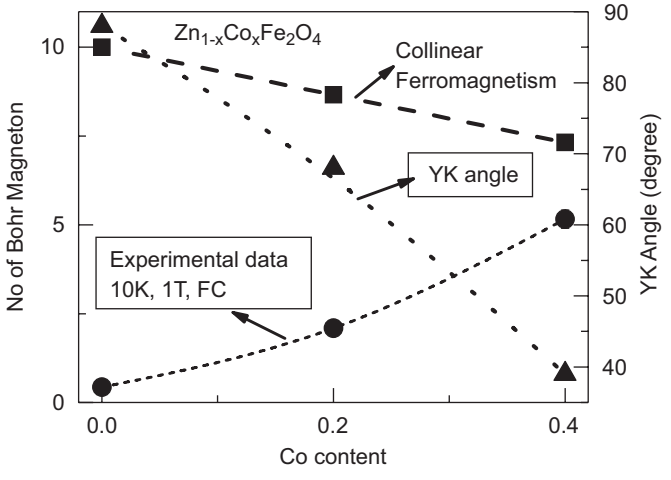

Fig. 6. The number of μ_B as a function of x for the $Zn_{1-x}Co_xFe_2O_4$. ■ indicates the predicted number of μ_B from the A and B sites cations for collinear ferromagnetism. ● indicates the experimental number of μ_B at 10 K. The YK angles (▲) are also shown in this figure.

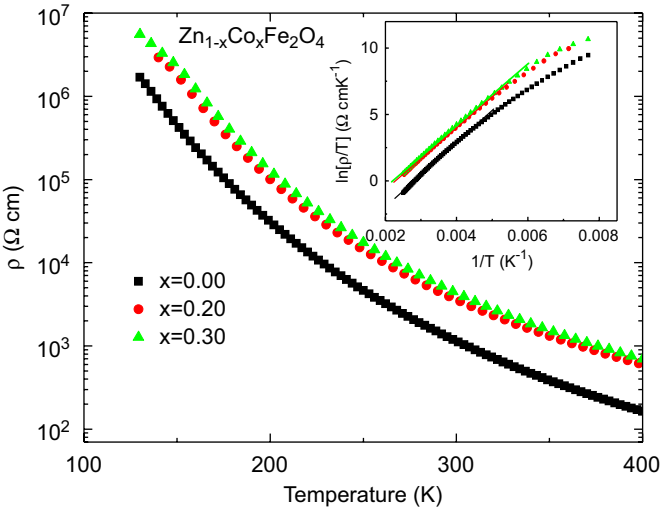

Fig. 7. Temperature dependence of resistivity for various $Zn_{1-x}Co_xFe_2O_4$ samples. The inset shows the fit to the polaron hopping model.

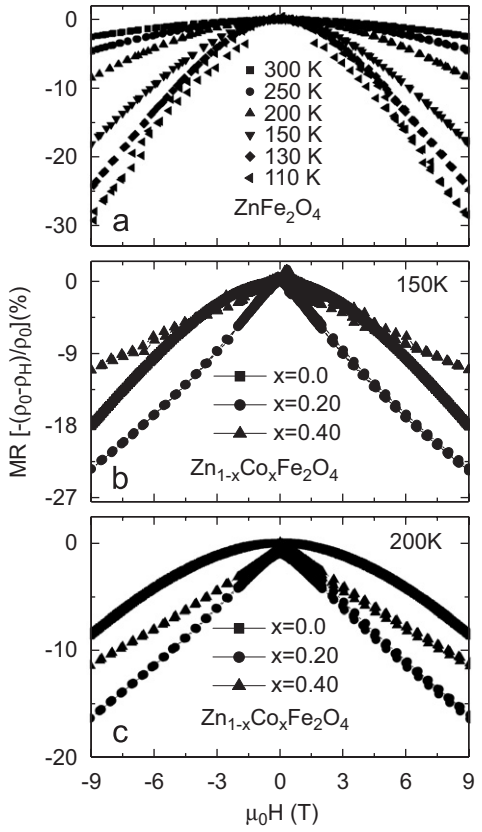

Fig. 8. Field dependence of MR for the (a) $ZnFe_2O_4$ at various temperatures, (b) $Zn_{1-x}Co_xFe_2O_4$ for $x = 0$, 0.20 and 0.40 at 150 K and (c) $Zn_{1-x}Co_xFe_2O_4$ for $x = 0$, 0.20 and 0.40 at 200 K.

materials [12], which follows the Inoue and Maekawa [22] model, $MR(\%) = C(M/M_s)^2$.

Fig. 8(b) and (c) shows the MR(H) loops for various $Zn_{1-x}Co_xFe_2O_4$ at 150 and 200 K, respectively. It is found that both MR values and shape of the MR loops vary as a function of Co content. At 150, 200 and 250 K (not shown), the shape of the MR(H) loop for the $ZnFe_2O_4$ is different from that of other Co-substituted $Zn_{1-x}Co_xFe_2O_4$. For the $ZnFe_2O_4$, MR(H) loops at all temperatures are parabolic in shape. At 300 K, the shapes of MR(H) loops for $ZnFe_2O_4$ and $Zn_{0.80}Co_{0.20}Fe_2O_4$ are similar, although the MR value depends on the composition. This is because at 300 K, $Zn_{0.80}Co_{0.20}Fe_2O_4$ is also in the paramagnetic (T_c~170 K) regime like the $ZnFe_2O_4$. In the ferrimagnetic regime, the shape of the MR(H) loops is almost linear with the field. No hysteresis is observed in the MR(H) loops.

Fig. 9 shows the MR(9 T) as a function of temperature for the various $Zn_{1-x}Co_xFe_2O_4$ samples. It is observed that MR is maximum for $x = 0.2$. The MR increases as the Co content in $Zn_{1-x}Co_xFe_2O_4$ increases up to $x = 0.2$ and then decreases for further increase of Co content. It is also observed that the mixed $Zn_{1-x}Co_xFe_2O_4$ ferrites for small Co concentration are not saturated at 10 K in the presence of 5 T field (see Fig. 4). Systematically investigated M data indicate a definite evidence of non-collinear (canted) arrangement of YK type in $Zn_{1-x}Co_xFe_2O_4$, for

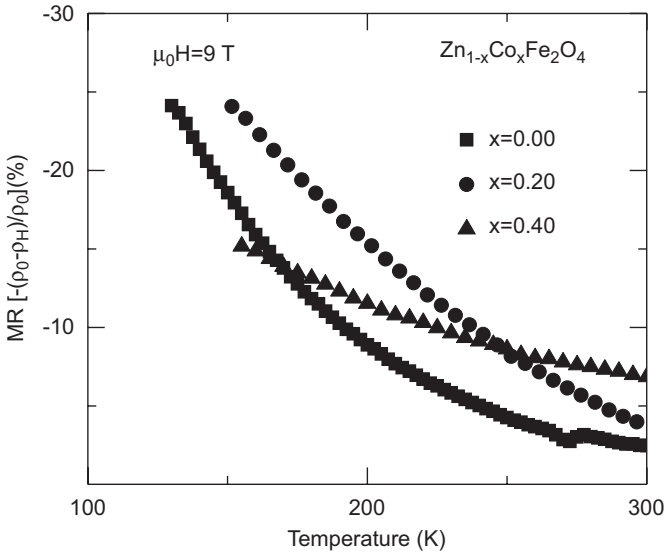

Fig. 9. Temperature dependence of MR(9 T) for the various $Zn_{1-x}Co_xFe_2O_4$ samples.

$x < 0.5$ [23]. On the other hand, for $x > 0.5$, almost all samples up to $CoFe_2O_4$ are collinear ferrimagnets. The MR observed in these samples is higher than that of the spinel Fe_3O_4 [16] or chalcogenide spinel [17].

From microstructural study it is found that variable grain sizes are produced in $ZnFe_2O_4$ samples sintered at various temperatures. The investigation of grain size dependence of MR in $ZnFe_2O_4$ shows that the MR is completely independent of the grain size, although their ρ values vary significantly as shown in Fig. 10. This fact indicates that the MR observed in these samples is not an extrinsic effect (related to the grain boundaries) as observed in manganites [12], rather this is an intrinsic effect.

The dM/dH and the MR depend on the Co content, and are found higher for $x = 0.2$. From these results, it is predicted that the MR is originated from the spin-canting state of the sample, i.e. the YK angle [1,18,23]. The YK angle, α_{YK}, can be estimated from the calculation of magnetic moments from A and B sites of spinel structure. From the previous neutron-diffraction data [1] and the Mossbauer spectroscopic data [3], the cation distribution in $Zn_{1-x}Co_xFe_2O_4$ ferrites follows $Zn_{1-x}Fe_x[Co_xFe_{2-x}]O_4$ for the various x values, where the second term within square bracket indicates the octahedral (B) sites and the first term indicates tetrahedral (A) sites. If we assume that the α_{YK} for the various B sites cations are the same, and the experimental saturation moment is $M_s(\mu_B)$, then the average α_{YK} as a function of x can be calculated from the following relation:

$$\cos \alpha_{YK} = \frac{M_s(\mu_B) + 5x(\mu_B)}{(10 - 1.7x)\mu_B}. \quad (2)$$

The α_{YK} for the various $Zn_{1-x}Co_xFe_2O_4$ at 10 K are calculated and presented in Fig. 6. It is observed that, other

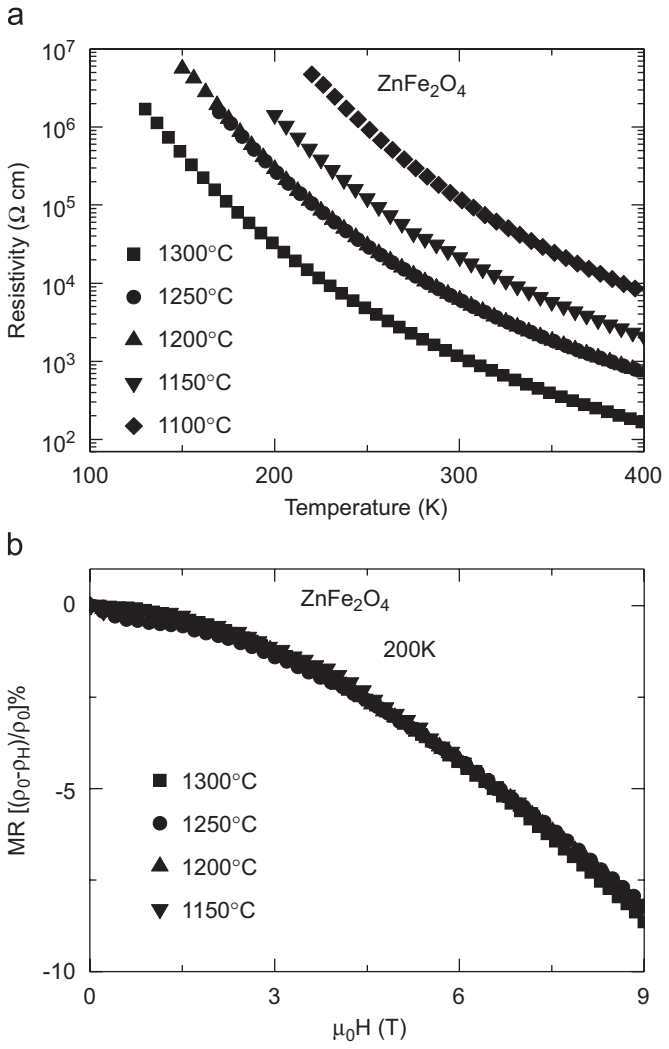

Fig. 10. (a) Temperature dependence of resistivity for $ZnFe_2O_4$ samples sintered at various sintering temperatures and (b) field dependence of MR at 200 K for various $ZnFe_2O_4$ samples.

than the $ZnFe_2O_4$ (which is paramagnetic), YK angle is higher for the $x = 0.2$ sample and hence it has the higher MR. Another possibility of origin of this MR observed in these samples may be due to the incomplete long-range ordering among magnetic ions. The applied magnetic field enhances the magnetic ordering and hence a decrease of resistance is observed in these samples.

4. Conclusions

The large negative MR effect is observed in the $ZnFe_2O_4$ and the Co-substituted $ZnFe_2O_4$ materials of the spinel structure. The MR(H) is either parabolic or linear depending on the Co contents and temperatures. The maximum MR is observed for $Zn_{0.80}Co_{0.20}Fe_2O_4$ polycrystalline sample. This MR effect is the intrinsic property of the materials and independent of the microstructures (grain size). The origin of the MR may be due to the suppression of the scattering of carriers from the paramagnetic spins or the canted spin (YK angle) or magnetic polaron. The MR is almost linear with applied magnetic field, making it suitable for magnetic sensor fabrication. The experimental studies suggest that bulk oxide materials other than mixed valent manganites and spinel $Zn_{1-x}Co_xFe_2O_4$ ferrites also exhibit MR. The MR can be enhanced and field scale can be reduced by using a sandwich structure ($NiFe_2O_4/Zn_{0.80}Co_{0.20}Fe_2O_4/NiFe_2O_4$) or by forming superlattices with the help of the pulsed laser deposition technique. Further studies in this direction are therefore needed.

Acknowledgment

The authors thank Dr. M. F. Mina, Department of Physics, Bangladesh University of Engineering and Technology, for his valuable suggestions for the preparation of the revised manuscript.

References

[1] N.S. Satya Murthy, M.G. Natera, S.I. Youssef, R.J. Begum, C.M. Srivastava, Phys. Rev. 181 (2) (1969) 969.
[2] V.C. Wilson, J.S. Kasper, Phys. Rev. 95 (6) (1954) 1408.
[3] L.K. Leung, B.J. Evans, A.H. Morish, Phys. Rev. B 8 (1) (1973) 29.
[4] J.M. Daniels, A. Rosencwaig, Can. J. Phys. 48 (4) (1970) 381.
[5] J.M. Hastings, L.M. Corliss, Phys. Rev. 102 (6) (1956) 1460.
[6] J.M. Hastings, L.M. Corliss, Rev. Mod. Phys. 25 (1) (1953) 114.
[7] B.N. Brockhouse, L.M. Corliss, J.M. Hastings, Phys. Rev. 98 (6) (1955) 1721.
[8] W. Schiessl, W. Potzel, H. Karzel, M. Steiner, G.M. Kalvius, A. Martin, M.K. Krause, I. Halevy, J. Gal, W. Schafer, G. Will, M. Hilberg, R. Wappling, Phys. Rev. B 53 (14) (1996) 9143.
[9] Y. Yamada, K. Kamazawa, T. Tsunoda, Phys. Rev. B 66 (2002) 064401.
[10] R. Valenzuela, Magnetic Ceramics, Cambridge University Press, Cambridge, 1994.
[11] A.P. Ramirez, J. Phys.: Condens. Matter 9 (1997) 8171.
[12] A.K.M. Akther Hossain, L.F. Cohen, F. Damay, A. Berenov, J. MacManus Driscoll, N. McN. Alford, N.D. Mathur, M.G. Blamire, J.E. Evetts, J. Magn. Magn. Mater. 192 (2) (1999) 263.
[13] S.C. Gausepohl, M. Lee, K. Char, R.A. Rao, C.B. Eom, Phys. Rev. B 52 (5) (1995) 3459.
[14] A. Mamchik, I.W. Chen, Appl. Phys. Lett. 82 (4) (2003) 613.
[15] H. Masumoto, Y. Shirakawa, Phys. Rev. 60 (1941) 835.
[16] S.B. Ogale, K. Ghosh, R.P. Sharama, R.L. Greene, R. Ramesh, T. Venkatesan, Phys. Rev. B 57 (13) (1998) 7823.
[17] A.P. Ramirez, R.J. Cava, J. Krajewski., Nature 386 (1997) 156.
[18] A.K.M. Akther Hossain, M. Seki, T. Kawai, H. Tabata, J. Appl. Phys. 96 (2004) 1273.
[19] L.J. van der Pauw, Philips Res. Rep. 13 (1) (1958) 1.
[20] L.J. van der Pauw, Philips Tech. Rev. 20 (8) (1958/59) 220.
[21] R.D. Shannon, Acta Crystallogr. A 32 (1976) 751.
[22] J. Inoue, S. Maekawa, Phys. Rev. B 53 (18) (1996) R11927.
[23] Y. Yafet, C. Kittel, Phys. Rev. B 4 (1971) 3912.
[24] G.A. Petitt, D.W. Forester, Phys. Rev. 87 (2) (1952) 290.
[25] R.N. Bhowmik, R. Ranganathan, J. Magn. Magn. Mater. 248 (2002) 101.